

# On $\Delta$ -Transforms

Júlia Borràs, Federico Thomas, *Member, IEEE*, and Carme Torras, *Member, IEEE*

**Abstract**—Any set of two legs in a Gough–Stewart platform sharing an attachment is defined as a  $\Delta$  component. This component links a point in the platform (base) to a line in the base (platform). Thus, if the two legs, which are involved in a  $\Delta$  component, are rearranged without altering the location of the line and the point in their base and platform local reference frames, the singularity locus of the Gough–Stewart platform remains the same, provided that no architectural singularities are introduced. Such leg rearrangements are defined as  $\Delta$ -transforms, and they can be applied sequentially and simultaneously. Although it may seem counterintuitive at first glance, the rearrangement of legs using simultaneous  $\Delta$ -transforms does not necessarily lead to leg configurations containing a  $\Delta$  component. As a consequence, the application of  $\Delta$ -transforms reveals itself as a simple, yet powerful, technique for the kinematic analysis of large families of Gough–Stewart platforms. It is also shown that these transforms shed new light on the characterization of architectural singularities and their associated self-motions.

**Index Terms**—Architectural singularities, Gough–Stewart platform, kinematic components, pure condition, self-motion.

## I. INTRODUCTION

NOWADAYS, the analysis of robot singularities is probably the most active research topic in kinematics. Donelan, from Victoria University of Wellington in New Zealand, maintains a database currently containing more than 830 publications on this topic [1]. Those devoted to the singularity analysis of parallel robots represent a steadily increasing number; however, while the pioneer works were of a general nature [2]–[5], most of the recent works tackle the analysis of particular parallel designs. In this context, the development of new mathematical tools for the singularity analysis of parallel robots, though

Manuscript received December 3, 2008; revised May 22, 2009. First published November 6, 2009; current version published December 8, 2009. This paper was recommended for publication by Associate Editor I. Bonev and Editor W. K. Chung upon evaluation of the reviewers' comments. This work was supported in part by the Catalan Research Commission, through the Robotics group, and the Spanish Ministry of Science and Innovation under the I+D Project DPI2007-60858.

The authors are with the Institut de Robòtica i Informàtica Industrial, Consejo Superior de Investigaciones Científicas, Universitat Politècnica de Catalunya, Llorens i Artigas 4-6, Barcelona 08028, Spain (e-mail: jborras@iri.upc.edu; fthomas@iri.upc.edu; ctorras@iri.upc.edu).

This paper has supplementary downloadable multimedia material available at <http://ieeexplore.ieee.org>, provided by the author. The material includes a maple worksheet for each of the examples appearing in the paper, with the detailed numerical computations. Furthermore, it also contains a video of the self-motions for each of the architecturally singular manipulators appearing in the three examples within the paper. The complete list of all the videos (including their sizes) and other files (i.e., Maple worksheets, Web versions, etc.), with their corresponding sizes, is reported. All maple worksheets (files .mw) work under Maple 10-12 or higher. All videos (files .wmv) can be played with Windows Media Player 10 or higher. Contact jborras@iri.upc.edu for further questions about this work.

Color versions of one or more of the figures in this paper are available online at <http://ieeexplore.ieee.org>.

Digital Object Identifier 10.1109/TRO.2009.2032956

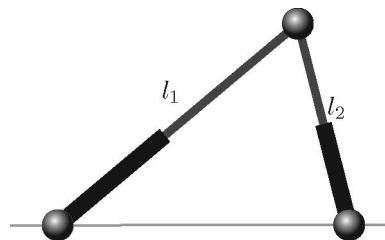


Fig. 1.  $\Delta$  component consists of two legs sharing one attachment.

difficult, is a must. This paper tries to contribute to this end by introducing the concept of  $\Delta$ -transform.

In general, substituting one leg of a Gough–Stewart platform by another arbitrary leg modifies the platform singularity locus in a rather unexpected way. Nevertheless, in those cases in which the considered platform contains rigid subassemblies, or *components* [6], legs can be rearranged so that the singularity locus is modified in a controlled way provided that the kinematics of the components is not changed [7].

The simplest component consists of two legs sharing a leg attachment, as shown in Fig. 1, which we will refer to as a  $\Delta$  component for obvious reasons. A  $\Delta$  component is rigid in the sense that, given the lengths of the two involved legs, a point in the platform (base) is rigidly linked to a line on the base (platform). A leg in a  $\Delta$  component can always be substituted by another leg connecting the point and the line without altering the location of the point with respect to the line and, hence, the kinematics of this component. In other words, the transformed  $\Delta$  component spans the same set of velocities as the original one, i.e., all those parallel to the plane formed by the attachment points, and in addition, there exists a one-to-one correspondence between both vectors fields. This simple observation is the basis for what is referred to as  $\Delta$ -transform.

The classification of Gough–Stewart platforms, which is on the basis of the components they contain, was addressed in [6]. Each class consists of all the manipulators, which are obtained by adding to a given component the remaining legs up to six in all possible topological configurations. Note that the manipulators in a class have neither the same forward kinematics nor the same singularity structure. The present work, on the contrary, tries to come up with a transformation that preserves the platform's singularities, thus opening up the possibility of classifying platforms in families sharing the same singularity structure. One such family of mechanisms, whose common tripod component leads them to share parallel singularities, has been studied in the context of composite serial in-parallel robots [9].

Two remarks that need to be considered here are as follows. First, we are dealing only with parallel singularities, which are relevant for the forward kinematic analysis of Gough–Stewart platforms. Hence, neither serial singularities nor constraint

wrenches arising in robots with less than 6 degrees of freedom (DOFs) are considered. Second, note that the leg rearrangements induced by a  $\Delta$ -transform do modify the Jacobian matrix (although not the zeros of its determinant). Thus, each new design that is obtained may behave differently near singularities.

The idea of using  $\Delta$ -transforms for the kinematic analysis of parallel platforms was first proposed, in a rather intuitive way, in [11] to generate the family of flagged parallel manipulators. Here, we formalize and extend this idea, thus introducing the possibility of applying these transformations simultaneously.

When the two legs in a  $\Delta$  component are made coincident by applying a  $\Delta$ -transform, a trivial architectural singularity is introduced [12]. In this paper, we show how applying a set of  $\Delta$ -transforms simultaneously leads to the possibility of introducing complex, nontrivial, architectural singularities. Obtaining architectural singular platforms in this way provides, as a by-product, a simple way to characterize their associated self-motions.

The polynomial expressions of the self-motion curves for some specializations of the Gough–Stewart platform have been solved either analytically [13], [14] or numerically using continuation [15], [16]. In contrast, here, we obtain a parameterization of such curves in configuration space, which are plotted in the workspace by solving the forward kinematics of a nonarchitectural singular platform whose leg lengths depend on a parameter.

This paper is structured as follows. Section II briefly reviews the characterization of singularities for Gough–Stewart platforms and the associated concept of pure condition. Section III introduces the concept of  $\Delta$ -transform and studies how its application modifies the pure condition of the analyzed platform. To show the potential of this transform for parallel platform kinematic analysis, Sections IV and V are devoted to the detailed analysis of the Zhang–Song and Griffis–Duffy platforms, respectively, which are based on the sequential and simultaneous application of  $\Delta$ -transforms. Section VI provides clues and hints to apply the presented transform to parallel platforms other than those of the Gough–Stewart type. Section VII summarizes the main contributions presented in this paper. Finally, the Appendix compiles basic facts on the concept of pure condition.

## II. SINGULARITIES OF GOUGH–STEWART PLATFORMS

Let us consider the general Gough–Stewart platform, as shown in Fig. 2, whose six linear actuators' lengths are given by  $l_1, \dots, l_6$ . In an abuse of language, legs will be denoted by their associated length variable. The linear actuators' velocities, which are given by  $\dot{l}_1, \dot{l}_2, \dots, \dot{l}_6$ , can be expressed in terms of the platform velocity vector  $(\mathbf{v}, \boldsymbol{\Omega})$  as follows:

$$\begin{pmatrix} \dot{l}_1 \\ \dot{l}_2 \\ \vdots \\ \dot{l}_6 \end{pmatrix} = \mathbf{K} \begin{pmatrix} \mathbf{v} \\ \boldsymbol{\Omega} \end{pmatrix} \quad (1)$$

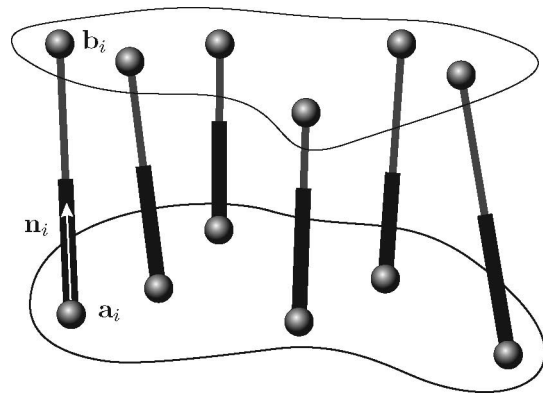


Fig. 2. General Gough–Stewart platform. Each leg  $l_i$ ,  $i = 1, \dots, 6$  is attached to the base and the platform at the points with global coordinates  $\mathbf{a}_i$  and  $\mathbf{b}_i$ , respectively, and  $\mathbf{n}_i$  is the unit free vector such that  $l_i \mathbf{n}_i = \mathbf{b}_i - \mathbf{a}_i$ .

with

$$\mathbf{K} = \begin{pmatrix} \mathbf{n}_1^T & (\mathbf{a}_1 \times \mathbf{n}_1)^T \\ \mathbf{n}_2^T & (\mathbf{a}_2 \times \mathbf{n}_2)^T \\ \vdots & \vdots \\ \mathbf{n}_6^T & (\mathbf{a}_6 \times \mathbf{n}_6)^T \end{pmatrix} \quad (2)$$

i.e., the matrix of Plücker coordinates of the six leg lines (for details, see [17]), where  $\mathbf{a}_i$  are the global coordinates of the attachment point of leg  $l_i$  to the base of the Gough–Stewart platform, and  $\mathbf{n}_i$  is the unit free vector anchored at  $\mathbf{a}_i$  and defining the orientation of leg  $l_i$ . Note that, in order to simplify notation, the same symbol is used to represent a point and its position vector.

The matrix  $\mathbf{K}$  can be factorized as follows:

$$\begin{aligned} \mathbf{K} &= \begin{pmatrix} 1/l_1 & 0 & \cdots & 0 \\ 0 & 1/l_2 & \cdots & 0 \\ \vdots & \vdots & \ddots & \vdots \\ 0 & 0 & \cdots & 1/l_6 \end{pmatrix} \\ &\quad \begin{pmatrix} (\mathbf{b}_1 - \mathbf{a}_1)^T & (\mathbf{a}_1 \times (\mathbf{b}_1 - \mathbf{a}_1))^T \\ (\mathbf{b}_2 - \mathbf{a}_2)^T & (\mathbf{a}_2 \times (\mathbf{b}_2 - \mathbf{a}_2))^T \\ \vdots & \vdots \\ (\mathbf{b}_6 - \mathbf{a}_6)^T & (\mathbf{a}_6 \times (\mathbf{b}_6 - \mathbf{a}_6))^T \end{pmatrix} \\ &= \text{diag}(1/l_1, 1/l_2, \dots, 1/l_6) \mathbf{P}. \end{aligned}$$

Then, the singularities of the platform are those configurations in which

$$\det(\mathbf{K}) = \frac{1}{l_1 l_2 l_3 l_4 l_5 l_6} \det(\mathbf{P}) = 0. \quad (3)$$

The dividing term is usually neglected because it is assumed that, in practice, leg lengths cannot be null. Thus, only the term  $\det(\mathbf{P})$  is considered, which can be expressed as products and additions of  $4 \times 4$  determinants, with each of them involving the homogenous coordinates of four different leg attachments [18]. The resulting expression, which will be called *pure expression*, can be greatly simplified for most well-known special Gough–Stewart platforms. For example, for the basic flagged and the octahedral Gough–Stewart platforms appearing in Fig. 3, the

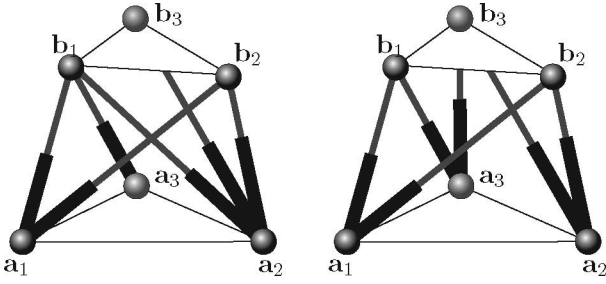


Fig. 3. Basic (left) flagged and (right) octahedral Gough–Stewart platforms.

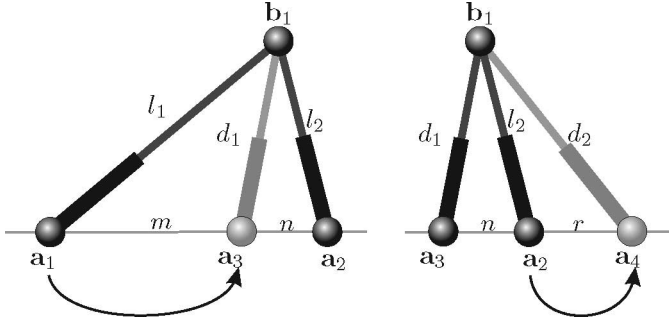


Fig. 4.  $\Delta$  component formed by legs  $l_1$  and  $l_2$ . Two  $\Delta$ -transforms can be applied to move the two attachments, which are  $a_1$  and  $a_2$ , along the line.

pure expression is given by

$$\begin{vmatrix} \mathbf{a}_1 & \mathbf{a}_2 & \mathbf{a}_3 & \mathbf{b}_1 \\ 1 & 1 & 1 & 1 \end{vmatrix} \begin{vmatrix} \mathbf{a}_1 & \mathbf{a}_2 & \mathbf{b}_1 & \mathbf{b}_2 \\ 1 & 1 & 1 & 1 \end{vmatrix} \begin{vmatrix} \mathbf{a}_2 & \mathbf{b}_1 & \mathbf{b}_2 & \mathbf{b}_3 \\ 1 & 1 & 1 & 1 \end{vmatrix} \quad (4)$$

and

$$\begin{vmatrix} \mathbf{b}_3 & \mathbf{a}_2 & \mathbf{a}_3 & \mathbf{b}_2 \\ 1 & 1 & 1 & 1 \end{vmatrix} \begin{vmatrix} \mathbf{b}_1 & \mathbf{a}_1 & \mathbf{a}_3 & \mathbf{b}_3 \\ 1 & 1 & 1 & 1 \end{vmatrix} \begin{vmatrix} \mathbf{b}_2 & \mathbf{a}_1 & \mathbf{a}_2 & \mathbf{b}_1 \\ 1 & 1 & 1 & 1 \end{vmatrix} \\ - \begin{vmatrix} \mathbf{b}_3 & \mathbf{a}_2 & \mathbf{a}_3 & \mathbf{b}_1 \\ 1 & 1 & 1 & 1 \end{vmatrix} \begin{vmatrix} \mathbf{b}_1 & \mathbf{a}_1 & \mathbf{a}_3 & \mathbf{b}_2 \\ 1 & 1 & 1 & 1 \end{vmatrix} \begin{vmatrix} \mathbf{b}_2 & \mathbf{a}_1 & \mathbf{a}_2 & \mathbf{b}_3 \\ 1 & 1 & 1 & 1 \end{vmatrix} \quad (5)$$

respectively [18]. These two expressions will be useful later, in Sections IV and V, respectively.

A pure expression, when equated to zero to characterize the configurations in which a given platform is singular, is known as a *pure condition* [46] (see the Appendix for a brief compilation of basic facts on the concept of pure condition).

### III. $\Delta$ -TRANSFORM

Let us consider a Gough–Stewart platform containing the  $\Delta$  component, which is defined by legs  $l_1$  and  $l_2$ , as shown on the left-hand side of Fig. 4. Now, let us introduce leg  $d_1$ , as shown in the same figure. Lengths  $l_1$ ,  $l_2$ , and  $d_1$  are not independent, and the relation between them can be straightforwardly obtained by realizing that the volume of the tetrahedron, which is defined by  $\mathbf{a}_1$ ,  $\mathbf{a}_2$ ,  $\mathbf{a}_3$ , and  $\mathbf{b}_1$ , is null, i.e., all four points are coplanar. Then, using Euler’s formula for the volume of a tetrahedron in terms of the square of its edge lengths [19, Problem 68], we

have

$$f(l_1, l_2, d_1) = \begin{vmatrix} 0 & 1 & 1 & 1 & 1 \\ 1 & 0 & (m+n)^2 & l_1^2 & m^2 \\ 1 & (m+n)^2 & 0 & l_2^2 & n^2 \\ 1 & l_1^2 & l_2^2 & 0 & d_1^2 \\ 1 & m^2 & n^2 & d_1^2 & 0 \end{vmatrix} = 0. \quad (6)$$

The aforementioned determinant can be recognized as the Cayley–Menger determinant of four points (for a review of these determinants and their generalizations, see [20]). The Cayley–Menger determinant of  $n$  points is proportional to the squared volume of the simplex that these points define in  $\mathbb{R}^{n-1}$ . This kind of determinants plays a fundamental role in the so-called *distance geometry*, which is a branch of geometry devoted to the characterization and study of sets of points on the basis of only their pairwise distances. Hence, distance geometry has immediate relevance where distances between points are determined or considered. It started to receive a lot of attention 20 years ago with the advent of molecular magnetic resonance experiments to obtain distances between atoms in rigid molecules [21] and, more recently, in robotics to obtain intrinsic formulations of different kinematics problems, thus avoiding the introduction of arbitrary reference frames [22], [23].

Now, (6) can be expressed as

$$f(l_1, l_2, d_1) = nl_1^2 + ml_2^2 - (m+n)d_1^2 - mn(m+n) = 0. \quad (7)$$

Thus, the time derivative of the leg length  $d_1$  can be expressed as

$$\dot{d}_1 = -\frac{\partial f/\partial l_1}{\partial f/\partial d_1} \dot{l}_1 - \frac{\partial f/\partial l_2}{\partial f/\partial d_1} \dot{l}_2 = \frac{l_1}{d_1} \frac{n}{m+n} \dot{l}_1 + \frac{l_2}{d_1} \frac{m}{m+n} \dot{l}_2. \quad (8)$$

Then, if we substitute leg  $l_1$  by leg  $d_1$ , the platform leg-length velocities after this substitution are given by

$$\begin{pmatrix} \dot{d}_1 \\ \dot{l}_2 \\ \vdots \\ \dot{l}_6 \end{pmatrix} = \begin{pmatrix} -\frac{\partial f/\partial l_1}{\partial f/\partial d_1} & \frac{\partial f/\partial l_2}{\partial f/\partial d_1} & \cdots & 0 \\ 0 & 1 & \cdots & 0 \\ \vdots & \vdots & \ddots & \vdots \\ 0 & 0 & \cdots & 1 \end{pmatrix} \begin{pmatrix} \dot{l}_1 \\ \dot{l}_2 \\ \vdots \\ \dot{l}_6 \end{pmatrix} \\ = \begin{pmatrix} \frac{l_1}{d_1} \frac{n}{m+n} & \frac{l_2}{d_1} \frac{m}{m+n} & \cdots & 0 \\ 0 & 1 & \cdots & 0 \\ \vdots & \vdots & \ddots & \vdots \\ 0 & 0 & \cdots & 1 \end{pmatrix} \begin{pmatrix} \dot{l}_1 \\ \dot{l}_2 \\ \vdots \\ \dot{l}_6 \end{pmatrix}. \quad (9)$$

The determinant of the previous matrix is given by

$$\frac{l_1}{d_1} \frac{n}{m+n}. \quad (10)$$

As a consequence, using (1) and (3), the pure expression of the platform after this leg substitution, say  $\det(\mathbf{P}_1)$ , can be expressed in terms of the pure expression of the original platform,

say  $\det(\mathbf{P}_0)$ , as

$$\det(\mathbf{P}_1) = \frac{n}{m+n} \cdot \det(\mathbf{P}_0). \quad (11)$$

Thus, the pure expression, after the substitution, is equal to the original one multiplied by the distance between the two attachments, divided by the same distance before the substitution, and affected by a sign change if the order of the attachments is permuted.

The previous substitution is defined as a  $\Delta$ -transform. In what follows, a  $\Delta$ -transform will be denoted by  $\Delta^{l_i, l_j, l_k}$ , which indicates that a  $\Delta$  component formed by  $l_i$  and  $l_j$  is substituted by the one formed by  $l_i$  and  $l_k$ .

By applying a  $\Delta$ -transform to a  $\Delta$  component, we have moved one of its two attachments on the line. We can move the other by applying one more  $\Delta$ -transform. For example, on the result of the previous  $\Delta$ -transform, we can substitute  $l_2$  by  $d_2$ , as shown in the right-hand side of Fig. 4. Then, following the same reasoning as for the first  $\Delta$ -transform, the pure expression of the resulting platform, say  $\det(\mathbf{P}_2)$ , can be expressed as

$$\det(\mathbf{P}_2) = \frac{n+r}{n} \cdot \det(\mathbf{P}_1) = \frac{n+r}{m+n} \cdot \det(\mathbf{P}_0). \quad (12)$$

Observe that we could apply the previous two  $\Delta$ -transforms simultaneously to move both attachments on the line at the same time. In this case, the relationship between the leg-length velocities can be expressed as

$$\begin{pmatrix} \dot{d}_1 \\ \dot{d}_2 \\ \dot{l}_3 \\ \vdots \\ \dot{l}_6 \end{pmatrix} = \begin{pmatrix} -\frac{\partial f_1/\partial l_1}{\partial f_1/\partial d_1} & -\frac{\partial f_1/\partial l_2}{\partial f_1/\partial d_1} & \cdots & 0 \\ -\frac{\partial f_2/\partial l_1}{\partial f_2/\partial d_2} & -\frac{\partial f_2/\partial l_2}{\partial f_2/\partial d_2} & \cdots & 0 \\ \vdots & \vdots & \ddots & \vdots \\ 0 & 0 & \cdots & 1 \end{pmatrix} \begin{pmatrix} \dot{l}_1 \\ \dot{l}_2 \\ \dot{l}_3 \\ \vdots \\ \dot{l}_6 \end{pmatrix}. \quad (13)$$

where

$$\begin{aligned} f_1(l_1, l_2, d_1) &= nl_1^2 + ml_2^2 - (m+n)d_1^2 - mn(m+n) = 0 \\ f_2(l_1, l_2, d_2) &= rl_1^2 + (m+n)d_2^2 - (m+n+r)l_2^2 \\ &\quad - r(m+n)(m+n+r) = 0. \end{aligned} \quad (14)$$

Computing the partial derivatives of these functions and substituting into (13), we obtain

$$\begin{pmatrix} \dot{d}_1 \\ \dot{d}_2 \\ \dot{l}_3 \\ \vdots \\ \dot{l}_6 \end{pmatrix} = \begin{pmatrix} \frac{l_1}{d_1} \frac{n}{m+n} & \frac{l_2}{d_1} \frac{m}{m+n} & \cdots & 0 \\ -\frac{l_1}{d_2} \frac{r}{m+n} & \frac{l_2}{d_2} \frac{m+n+r}{m+n} & \cdots & 0 \\ \vdots & \vdots & \ddots & \vdots \\ 0 & 0 & \cdots & 1 \end{pmatrix} \begin{pmatrix} \dot{l}_1 \\ \dot{l}_2 \\ \dot{l}_3 \\ \vdots \\ \dot{l}_6 \end{pmatrix}. \quad (15)$$

The determinant of the matrix in (15) is given by

$$\frac{l_1 l_2}{d_1 d_2} \frac{n(m+n+r) + mr}{(m+n)^2}$$

which easily simplifies to

$$\frac{l_1 l_2}{d_1 d_2} \cdot \frac{n+r}{m+n}. \quad (16)$$

Then, using (1) and (3), we can conclude that the pure expression of the platform after this double leg substitution can be expressed, as given in (12). Thus, the result is obviously the same if we apply the two  $\Delta$ -transforms either sequentially or simultaneously. Nevertheless, there are some circumstances in which a set of  $\Delta$ -transforms can only be applied simultaneously. This will become evident in the next two sections.

In what follows, a set of  $\Delta$ -transforms will be denoted by

$$\{\Delta^{l_1, l_2, l_3} \Delta^{l_4, l_5, l_6} \dots\}$$

when applied sequentially and by

$$\left\{ \begin{array}{c} \Delta^{l_1, l_2, l_3} \\ \Delta^{l_4, l_5, l_6} \\ \vdots \end{array} \right\}$$

when applied simultaneously.

#### IV. EXAMPLE I: ZHANG–SONG PLATFORM

Zhang and Song [24] identified an entire family of special Gough–Stewart platforms with closed-form formulation for their forward kinematics. One member of this family appears in Fig. 5(d), which is of interest because it has five aligned attachments, both in the base and the platform. Next, we will show that the pure condition of this platform is equal to that of the basic flagged platform, as shown in Fig. 3(a) (also known as 3-2-1) multiplied by a constant factor. To this end, let us first apply the sequence of  $\Delta$ -transforms to the basic flagged platform shown in Fig. 5(a)

$$\{\Delta^{p_1, p_3, q_3} \Delta^{p_2, p_4, q_4}\}$$

which leads to the platform shown in Fig. 5(b). Now, let us apply the sequence

$$\{\Delta^{q_1, q_2, l_2} \Delta^{q_3, q_4, l_4}\}$$

which leads to the platform shown in Fig. 5(c).

Therefore, it can be checked that, using (11) four times, the pure expression of the platform shown in Fig. 5(c) is that of the basic flagged platform shown in Fig. 5(a), i.e.,

$$\left| \begin{array}{cccc} \mathbf{a}_1 & \mathbf{a}_5 & \mathbf{a}_6 & \mathbf{b}_5 \\ 1 & 1 & 1 & 1 \end{array} \right| \left| \begin{array}{cccc} \mathbf{a}_1 & \mathbf{a}_6 & \mathbf{b}_2 & \mathbf{b}_5 \\ 1 & 1 & 1 & 1 \end{array} \right| \left| \begin{array}{cccc} \mathbf{a}_6 & \mathbf{b}_2 & \mathbf{b}_5 & \mathbf{b}_6 \\ 1 & 1 & 1 & 1 \end{array} \right| \quad (17)$$

multiplied by

$$\frac{n_1^2 (m_2 + n_2 + r_2)^2}{n_{11}^2 (m_2 + n_{21})^2}. \quad (18)$$

Now, let us apply the simultaneous set of  $\Delta$ -transforms

$$\left\{ \begin{array}{c} \Delta^{l_3 l_1 d_1} \\ \Delta^{l_1 l_2 d_2} \\ \Delta^{l_4 l_3 d_3} \\ \Delta^{l_2 l_4 d_4} \end{array} \right\}.$$

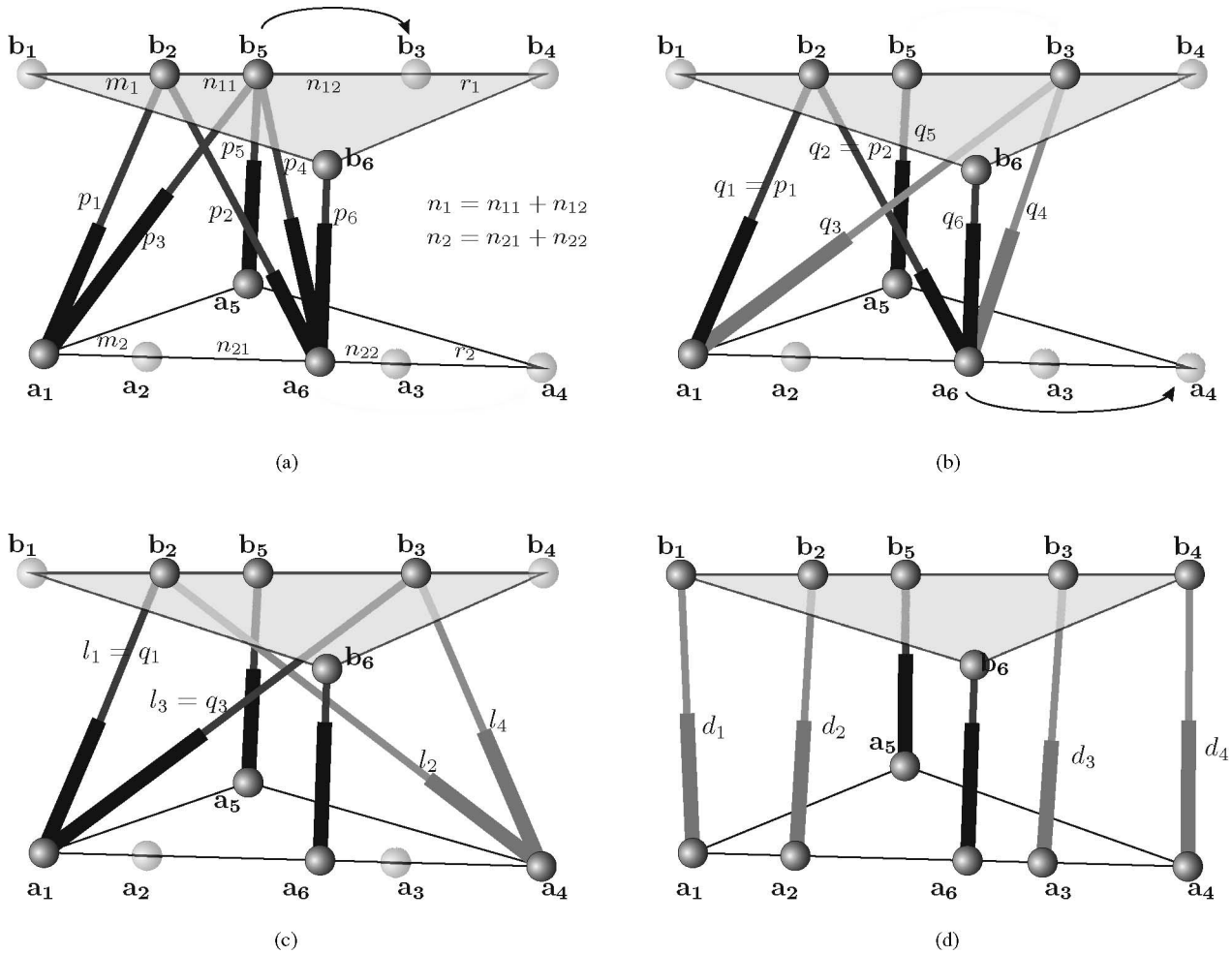


Fig. 5. Basic flagged platform in (a) can be transformed through a set of  $\Delta$ -transforms into the Zhang–Song platform in (d).

This set of  $\Delta$ -transforms is characterized by the following linear relation:

$$\begin{pmatrix} \dot{d}_1 \\ \dot{d}_2 \\ \dot{d}_3 \\ \dot{d}_4 \end{pmatrix} = \begin{pmatrix} \frac{\partial f_1/\partial l_1}{\partial f_1/\partial d_1} & 0 & \frac{\partial f_1/\partial l_3}{\partial f_1/\partial d_1} & 0 \\ \frac{\partial f_2/\partial l_1}{\partial f_2/\partial d_2} & \frac{\partial f_2/\partial l_2}{\partial f_2/\partial d_2} & 0 & 0 \\ 0 & 0 & \frac{\partial f_3/\partial l_3}{\partial f_3/\partial d_3} & \frac{\partial f_3/\partial l_4}{\partial f_3/\partial d_3} \\ 0 & \frac{\partial f_4/\partial l_2}{\partial f_4/\partial d_4} & 0 & \frac{\partial f_4/\partial l_4}{\partial f_4/\partial d_4} \end{pmatrix} \begin{pmatrix} \dot{l}_1 \\ \dot{l}_2 \\ \dot{l}_3 \\ \dot{l}_4 \end{pmatrix} \quad (19)$$

where

$$\begin{aligned} f_1 &= (m_1 + n_1)l_1^2 + n_1d_1^2 + m_1l_3^2 - m_1n_1(n_1 + m_1) \\ f_2 &= (n_2 + r_2)l_1^2 + m_2l_2^2 - (m_2 + n_2 + r_2)d_2^2 \\ &\quad - m_2(n_2 + r_2)(m_2 + n_2 + r_2) \end{aligned}$$

$$\begin{aligned} f_3 &= (m_2 + n_2)l_4^2 + r_2l_3^2 - (m_2 + n_2 + r_2)d_3^2 \\ &\quad - r_2(m_2 + n_2)(m_2 + n_2 + r_2) \\ f_4 &= r_1l_2^2 + n_1d_4^2 - (n_1 + r_1)l_4^2 - r_1n_1(r_1 + n_1). \end{aligned} \quad (20)$$

The determinant of the matrix in (19), after computing the corresponding derivatives, is given by

$$\frac{(m_1 + n_1)(n_1 + r_1)m_2r_2 - (n_2 + r_2)(m_2 + n_2)r_1m_1}{n_1^2(m_2 + n_2 + r_2)^2}. \quad (21)$$

As a consequence, the pure expression of the platform, which is shown in Fig. 5(d), is the product of factors (17), (18), and (21).

It is important to realize that factor (21) vanishes if, and only if

$$\frac{|a_3 - a_1||a_2 - a_4|}{|a_1 - a_2||a_3 - a_4|} = \frac{|b_3 - b_1||b_2 - b_4|}{|b_1 - b_2||b_3 - b_4|} \quad (22)$$

i.e., if the cross-ratio [25] of  $a_1, a_4, a_3$ , and  $a_2$  equals that of  $b_1, b_4, b_3$ , and  $b_2$ . When this happens, the pure expression of the Zhang–Song platform, which is shown in Fig. 5(d), is identically zero. In this case, the platform is said to be *architecturally singular*, i.e., it is always in a singularity independently of its leg lengths. Alternatively, it is also said that the platform exhibits

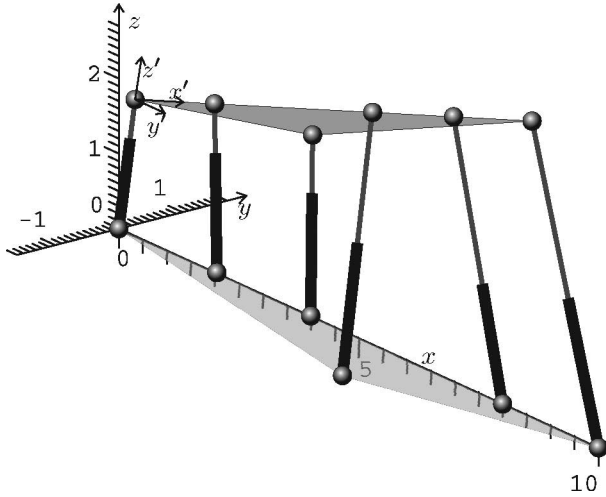


Fig. 6. Architecturally singular Zhang–Song platform, which is given in Table I, represented in one of its infinitely many possible configurations.

TABLE I

COORDINATES OF THE ATTACHMENTS IN THEIR LOCAL REFERENCE FRAMES FOR AN ARCHITECTURALLY SINGULAR ZHANG–SONG PLATFORM AND LEG LENGTHS FOR WHICH ITS SELF-MOTION IS ANALYZED (WHICH IS DRAWN IN FIG. 6)

$i$	$\mathbf{a}_i$	$\mathbf{b}_i$	$d_i^2$
1	(0, 0, 0)	(0, 0, 0)	22
2	(2, 0, 0)	(1, 0, 0)	$15 - \sqrt{2}$
3	(8, 0, 0)	(4, 0, 0)	$54 - 28\sqrt{2}$
4	(10, 0, 0)	(5, 0, 0)	$87 - 45\sqrt{2}$
5	(6, -1, 0)	(3, 0, 0)	$28 - 12\sqrt{2}$
6	(4, 0, 0)	(2, 2, 0)	$16 - (6 + \sqrt{3})\sqrt{2}$

a *self-motion*, i.e., it is movable while keeping its leg lengths constant. This architectural singularity corresponds to the line–line singular component studied in [26], and it also appears as the fifth type of singularity in [27, Th. 1] (or equivalently in [28, type 8 in Th. 3]). The cross-ratio singularity condition was also found in [29] and [30], using much more involved derivations than the one mentioned previously.

A parameterization of the self-motions resulting from architectural singularities introduced by a sequence of  $\Delta$ -transforms can always be found by proceeding backward, i.e., by undoing the  $\Delta$ -transforms and introducing parameters when needed. For example, for the Zhang–Song platform (see Fig. 6) with the leg-attachment coordinates appearing in Table I, the cross-ratio condition in (22) is satisfied. Hence, the platform is architecturally singular and, as a consequence, it will exhibit a self-motion. To obtain a parameterization of this self-motion, observe that, for the Zhang–Song architecturally singular platform, using (20), it can be concluded that

$$\begin{pmatrix} -4 & 0 & 1 & 0 \\ 8 & 2 & 0 & 0 \\ 0 & 0 & 2 & 8 \\ 0 & 1 & 0 & -4 \end{pmatrix} \begin{pmatrix} l_1^2 \\ l_2^2 \\ l_3^2 \\ l_4^2 \end{pmatrix} = \begin{pmatrix} 12 - 3d_1^2 \\ 160 + 10d_2^2 \\ 160 + 10d_3^2 \\ 12 - 3d_4^2 \end{pmatrix}. \quad (23)$$

Given fixed values for  $d_1^2, \dots, d_4^2$ , the previous linear system is underconstrained, as expected. In other words, there is an

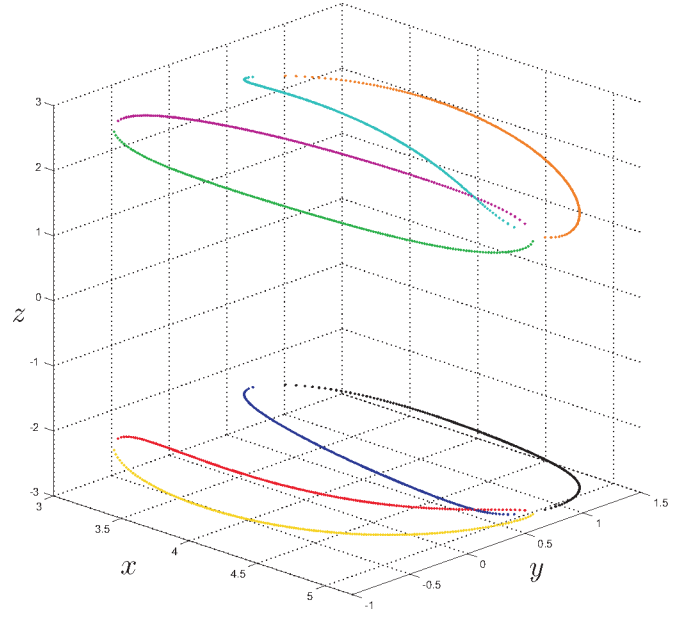


Fig. 7. Curve traced by the barycenter of the triangular platform, which is shown in Fig. 6, when it is moved along its self-motion. Each color corresponds to one branch of the forward kinematics generated as the parameter is swept.

infinite set of values for  $l_1^2, \dots, l_4^2$ , which are compatible with a set of values for  $d_1^2, \dots, d_4^2$ . This set can be parameterized, for the values of  $d_i^2$  in Table I, by taking one of the leg lengths as parameter ( $l_4^2$  has been chosen here), yielding

$$\begin{aligned} l_1^2 &= -l_4^2 + 101 - 35\sqrt{2} \\ l_2^2 &= 4l_4^2 - 249 + 135\sqrt{2} \\ l_3^2 &= -4l_4^2 + 350 - 140\sqrt{2}. \end{aligned} \quad (24)$$

We can proceed to undo the four other  $\Delta$ -transforms to obtain the leg lengths for the corresponding basic flagged parallel platform shown in Fig. 5(a). The result is given by

$$\begin{aligned} p_1^2 &= 101 - 35\sqrt{2} - l_4^2 \\ p_2^2 &= -63 + 33\sqrt{2} + l_4^2 \\ p_3^2 &= -3l_4^2 + 265 - 105\sqrt{2} \\ p_4^2 &= -l_4^2 + 101 - 45\sqrt{2} \\ p_5^2 &= 28 - 12\sqrt{2} \\ p_6^2 &= 16 - (6 + \sqrt{3})\sqrt{2}. \end{aligned} \quad (25)$$

The basic flagged parallel platform can have up to eight assembly modes that can be expressed in closed form in terms of its leg lengths [11]. Thus, by sweeping  $l_4^2$  in the range  $(0, \infty)$ , eight curves in the configuration space of the platform are traced. This provides a complete characterization of the sought self-motion. Fig. 7 depicts the location of the barycenter of the triangular moving platform for the obtained self-motion. For the computational steps in detail, see a Maple worksheet attached as a multimedia file with this paper.

Each value of the parameter  $l_4^2$  defines a unique point in joint space (a set of leg lengths), which leads to eight solutions of

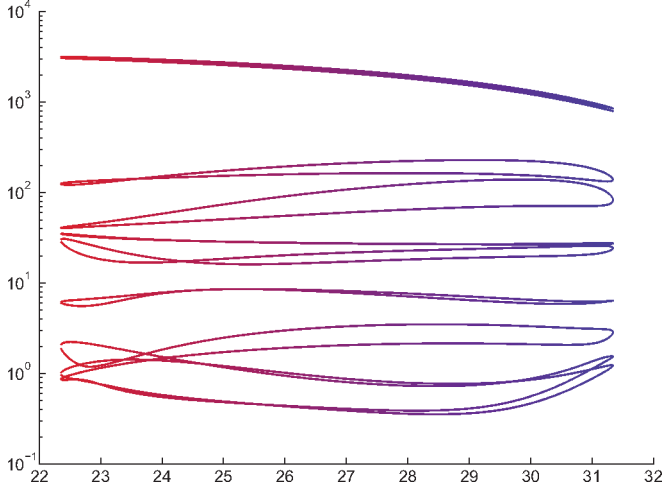


Fig. 8. All eigenvalues for all assembly modes, excluding the one that is always zero, of  $\mathbf{J}^T \mathbf{J}$ , where  $\mathbf{J}$  is the Jacobian matrix of the analyzed architecturally singular Zhang–Song platform, as a function of  $l_4^2$ .

the forward kinematics (one for each assembly mode) in configuration space. Note that these solutions may be real only for some ranges of the parameter. In the example, the parameter in the interval  $(22.35, 31.34)$  yields the real solutions plotted in Fig. 7. The extremes of this interval correspond to transition points between different assembly modes (which are marked with a change of color in the figure). Nevertheless, such transition points do not correspond to higher order singularities of the architecturally singular Zhang–Song platform. Indeed, if the eigenvalues of  $\mathbf{J}\mathbf{J}^T$ , where  $\mathbf{J}$  is the Jacobian matrix of the architecturally singular Zhang–Song platform, are computed along its self-motion, five of them are always different from zero. Fig. 8 plots all eigenvalues in logarithmic scale, excluding the one that is always zero, for all assembly modes, as a function of  $l_4^2$ . Note that none of them vanishes.

## V. EXAMPLE II: GRIFFIS–DUFFY PLATFORM

Let us consider the octahedral parallel platform shown in the top portion of Fig. 9, which is also known as 2-2-2 platform, whose pure expression is given by

$$\begin{aligned} & \left| \begin{array}{cccc} \mathbf{b}_5 & \mathbf{a}_4 & \mathbf{a}_6 & \mathbf{b}_3 \\ 1 & 1 & 1 & 1 \end{array} \right| \left| \begin{array}{cccc} \mathbf{b}_1 & \mathbf{a}_2 & \mathbf{a}_6 & \mathbf{b}_5 \\ 1 & 1 & 1 & 1 \end{array} \right| \left| \begin{array}{cccc} \mathbf{b}_3 & \mathbf{a}_2 & \mathbf{a}_4 & \mathbf{b}_1 \\ 1 & 1 & 1 & 1 \end{array} \right| \\ & - \left| \begin{array}{cccc} \mathbf{b}_5 & \mathbf{a}_4 & \mathbf{a}_6 & \mathbf{b}_1 \\ 1 & 1 & 1 & 1 \end{array} \right| \left| \begin{array}{cccc} \mathbf{b}_1 & \mathbf{a}_2 & \mathbf{a}_6 & \mathbf{b}_3 \\ 1 & 1 & 1 & 1 \end{array} \right| \left| \begin{array}{cccc} \mathbf{b}_3 & \mathbf{a}_2 & \mathbf{a}_4 & \mathbf{b}_5 \\ 1 & 1 & 1 & 1 \end{array} \right|. \end{aligned} \quad (26)$$

Now, applying to it the following set of  $\Delta$ -transforms:

$$\left\{ \begin{array}{l} \Delta^{l_2, l_1, d_1} \\ \Delta^{l_3, l_2, d_2} \\ \Delta^{l_4, l_3, d_3} \\ \Delta^{l_5, l_4, d_4} \\ \Delta^{l_6, l_5, d_5} \\ \Delta^{l_1, l_6, d_6} \end{array} \right\} \quad (27)$$

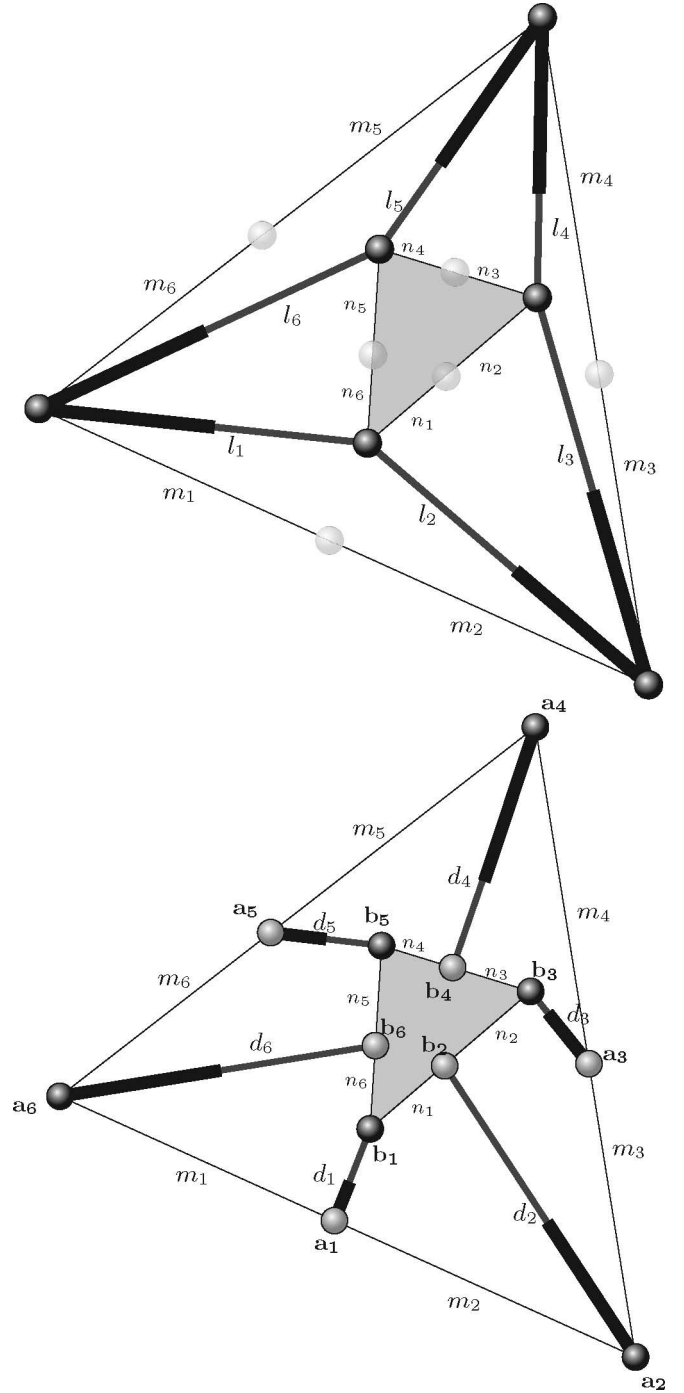


Fig. 9. Simultaneous application of six  $\Delta$ -transforms allows us to transform an (top) octahedral platform into a (bottom) Griffis–Duffy platform.

we have that the resulting platform is the Griffis–Duffy platform [31], which appears in the bottom portion of Fig. 9 (for a complete analysis of this special Gough–Stewart platform, see [32]).

The transformation matrix between the leg lengths velocities associated with the set of  $\Delta$ -transforms in (27) is given by (28), shown at the bottom of the next page, where

$$\begin{aligned} f_1 &= m_1 l_2^2 + m_2 l_1^2 - (m_1 + m_2) d_1^2 - m_1 m_2 (m_1 + m_2) \\ f_2 &= n_2 l_2^2 + n_1 l_3^2 - (n_1 + n_2) d_2^2 - n_1 n_2 (n_1 + n_2) \end{aligned}$$

$$\begin{aligned}
f_3 &= m_3 l_4^2 + m_4 l_3^2 - (m_3 + m_4) d_3^2 - m_3 m_4 (m_3 + m_4) \\
f_4 &= n_4 l_5^2 + n_3 l_4^2 - (n_3 + n_4) d_4^2 - n_3 n_4 (n_3 + n_4) \\
f_5 &= m_5 l_6^2 + m_6 l_5^2 - (m_5 + m_6) d_5^2 - m_5 m_6 (m_5 + m_6) \\
f_6 &= n_6 l_6^2 + n_5 l_1^2 - (n_6 + n_5) d_6^2 - n_6 n_5 (n_5 + n_6). \quad (29)
\end{aligned}$$

After computing the corresponding derivatives, the determinant of the matrix in (28) is given as in (30), shown at the bottom of this page.

Therefore, the pure expression of the platform shown in the bottom portion of Fig. 9 is that of the one shown in the top portion of Fig. 9 multiplied by factor (30). Note that this factor is constant, which only depends on architectural parameters.

It is easy to check that factor (30) vanishes if, and only if

$$\frac{|\mathbf{a}_2, \mathbf{a}_6, \mathbf{a}_3| |\mathbf{a}_1, \mathbf{a}_5, \mathbf{a}_4|}{|\mathbf{a}_2, \mathbf{a}_6, \mathbf{a}_4| |\mathbf{a}_1, \mathbf{a}_5, \mathbf{a}_3|} = \frac{|\mathbf{b}_2, \mathbf{b}_6, \mathbf{b}_3| |\mathbf{b}_1, \mathbf{b}_5, \mathbf{b}_4|}{|\mathbf{b}_2, \mathbf{b}_6, \mathbf{b}_4| |\mathbf{b}_1, \mathbf{b}_5, \mathbf{b}_3|} \quad (31)$$

where  $|\mathbf{a}_i, \mathbf{a}_j, \mathbf{a}_k|$  is the area of the triangle defined by points  $\mathbf{a}_i, \mathbf{a}_j$ , and  $\mathbf{a}_k$ . It is worth noting that these cross-ratios between areas are projective invariants whose role for coplanar points is similar to that of the cross-ratios between distances for collinear points [33].

Using rather more complicated arguments, the algebraic condition derived from factor (30) to detect architectural singularities in Griffis–Duffy platforms was already found in [32]. In this latter reference, the reader can also find an alternative geometric interpretation, which, from our point of view, is not as elegant as the one given previously in terms of cross-ratios between areas. Another interpretation of the same factor (30) can be found in [34]. The same manipulator was used in [35] as a particular case example of a general theorem on architectural singularities.

An important consequence of this result is that, if factor (30) is different from zero, the singularity locus of a Griffis–Duffy platform is the same as that of an octahedral platform. If it is zero, the platform is architecturally singular.

As an example of architecturally singular Griffis–Duffy platform, consider the platform with the leg-attachment coordinates

TABLE II  
COORDINATES OF THE ATTACHMENTS IN THEIR LOCAL REFERENCE FRAMES FOR AN ARCHITECTURALLY SINGULAR GRIFFIS–DUFFY PLATFORM, AND LEG LENGTHS FOR WHICH ITS SELF-MOTION IS ANALYZED (WHICH IS DRAWN IN FIG. 10)

$i$	$\mathbf{a}_i$	$\mathbf{b}_i$	$d_i^2$
1	(0, 0, 0)	(0, $\sqrt{3}$ , 0)	$3 - \sqrt{3}$
2	(2, 0, 0)	(-1/2, $\sqrt{3}/2$ , 0)	2
3	(1, $\sqrt{3}$ , 0)	(-1, 0, 0)	$5 - \sqrt{3}$
4	(0, $2\sqrt{3}$ , 0)	(0, 0, 0)	$15 - 4\sqrt{3}$
5	(-1, $\sqrt{3}$ , 0)	(1, 0, 0)	$11 - 5\sqrt{3}$
6	(-2, 0, 0)	(1/2, $\sqrt{3}/2$ , 0)	$11 - 3\sqrt{3}$

appearing in Table II (see Fig. 10). In this case factor (30) is identically zero. Hence, the platform is architecturally singular and, as a consequence, it will exhibit a self-motion. To obtain a characterization of this self-motion, we will proceed as in the previous section. First, observe that, for the Griffis–Duffy architecturally singular platform, using the system of equations in (29), it can be concluded that

$$\begin{pmatrix} 2 & 2 & 0 & 0 & 0 & 0 \\ 0 & 1 & 1 & 0 & 0 & 0 \\ 0 & 0 & 2 & 2 & 0 & 0 \\ 0 & 0 & 0 & 1 & 1 & 0 \\ 0 & 0 & 0 & 0 & 2 & 2 \\ 1 & 0 & 0 & 0 & 0 & 1 \end{pmatrix} \begin{pmatrix} l_1^2 \\ l_2^2 \\ l_3^2 \\ l_4^2 \\ l_5^2 \\ l_6^2 \end{pmatrix} = \begin{pmatrix} 16 + 4d_1^2 \\ 2 + 2d_2^2 \\ 16 + 4d_3^2 \\ 2 + 2d_4^2 \\ 16 + 4d_5^2 \\ 2 + 2d_6^2 \end{pmatrix}. \quad (32)$$

Since the previous matrix is rank-defective, there is an infinite number of values for  $l_1^2, \dots, l_6^2$ , which are compatible with  $d_1^2, \dots, d_6^2$ . Substituting the values of  $d_1^2, \dots, d_6^2$  in Table II and solving the previous system taking  $l_6^2$  as parameter, we get

$$\begin{aligned}
l_1^2 &= -l_6^2 + 24 - 6\sqrt{3} \\
l_2^2 &= l_6^2 - 10 + 4\sqrt{3}
\end{aligned}$$

$$\begin{pmatrix} \frac{\partial f_1}{\partial l_1} & \frac{\partial f_1}{\partial l_2} & 0 & 0 & 0 & 0 \\ \frac{\partial f_1}{\partial d_1} & \frac{\partial f_1}{\partial d_1} & 0 & 0 & 0 & 0 \\ 0 & \frac{\partial f_2}{\partial l_2} & \frac{\partial f_2}{\partial l_3} & 0 & 0 & 0 \\ & \frac{\partial f_2}{\partial d_2} & \frac{\partial f_2}{\partial d_2} & & & \\ 0 & 0 & \frac{\partial f_3}{\partial l_3} & \frac{\partial f_3}{\partial l_4} & 0 & 0 \\ & & \frac{\partial f_3}{\partial d_3} & \frac{\partial f_3}{\partial d_3} & & \\ 0 & 0 & 0 & \frac{\partial f_4}{\partial l_4} & \frac{\partial f_4}{\partial l_5} & 0 \\ & & & \frac{\partial f_4}{\partial d_4} & \frac{\partial f_4}{\partial d_4} & \\ 0 & 0 & 0 & 0 & \frac{\partial f_5}{\partial l_5} & \frac{\partial f_5}{\partial l_6} \\ & & & & \frac{\partial f_5}{\partial d_5} & \frac{\partial f_5}{\partial d_5} \\ \frac{\partial f_6}{\partial l_1} & 0 & 0 & 0 & 0 & \frac{\partial f_6}{\partial l_6} \\ \frac{\partial f_6}{\partial d_6} & 0 & 0 & 0 & 0 & \frac{\partial f_6}{\partial d_6} \end{pmatrix} \quad (28)$$

$$\frac{m_2 m_4 m_6 n_2 n_4 n_6 - m_1 m_3 m_5 n_1 n_3 n_5}{(m_1 + m_2)(m_3 + m_4)(m_5 + m_6)(n_1 + n_2)(n_3 + n_4)(n_5 + n_6)} \quad (30)$$



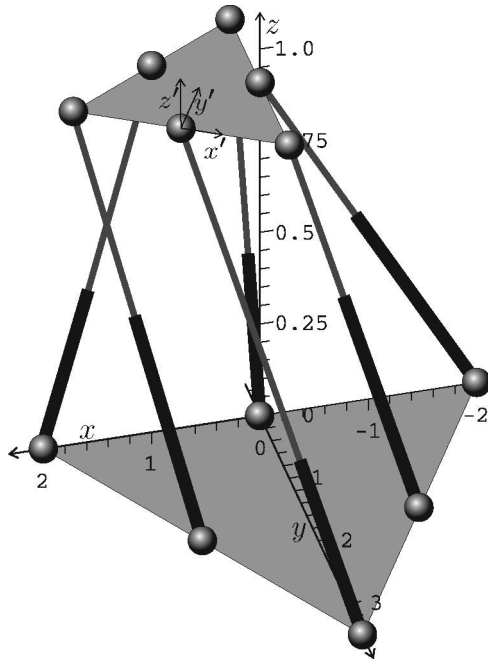


Fig. 10. Architecturally singular Griffis–Duffy platform, which is given in Table II, represented in one of its infinitely many possible configurations.

$$\begin{aligned} l_3^2 &= -l_6^2 + 16 - 4\sqrt{3} \\ l_4^2 &= l_6^2 + 2 + 2\sqrt{3} \\ l_5^2 &= -l_6^2 + 30 - 10\sqrt{3}. \end{aligned} \quad (33)$$

The octahedral platform can have up to 16 assembly modes that can be obtained as the roots of an eight-degree polynomial in the square of the unknown [36, p. 161]. Thus, no algebraic formula exists for the forward kinematics of the octahedral platform. Nevertheless, the self-motion can be characterized by sweeping  $l_6^2$  in the range  $(0, \infty)$  and obtaining the roots of the biotic polynomial numerically. The 16 solutions obtained for each value of  $l_6^2$  form eight pairs of manipulator postures, with one being the mirror image of another about the base plane.

Fig. 11 shows the location of the barycenter of the triangular moving platform for the obtained self-motion. The parameter is swept from its lowest value (discontinuities on the top, bottom, and right on the figure) to its uppermost value (discontinuities in the center of the figure). It is interesting to note that four assembly modes are real for  $l_6^2 \in (3.89, 6.025)$ , and eight are real for  $l_6^2 \in (6.025, 8.9)$ . The platform cannot be assembled for  $l_6^2$ , which is outside the range  $(3.89, 8.9)$ . As in the example of the previous section, the configurations obtained for the value of the parameter that lead to changes in the number of assembly modes do not correspond to higher order singularities of the architecturally singular platform. Indeed, if the eigenvalues of  $\mathbf{J}\mathbf{J}^T$ , where  $\mathbf{J}$  is the Jacobian matrix of the architecturally singular Griffis–Duffy platform, are computed along the self-motion, five of them are always different from zero. Fig. 12 plots all eigenvalues in logarithmic scale, excluding the one that is always zero, for all assembly modes, as a function of the chosen parameter. Note that none of them vanishes.

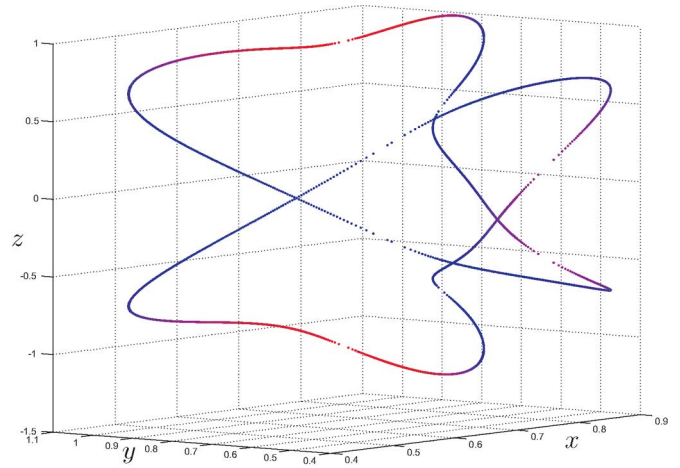


Fig. 11. Curve traced by the barycenter of the triangular platform, which is shown in Fig. 10, when it is moved along its self-motion. The parameter is swept from its lowest value (discontinuities on the top, bottom, and right on the figure) to its uppermost value (discontinuities in the center of the figure). In the color version of the plot, this is displayed as changing from red (lower values) to blue (upper values). The curve consists of two symmetric disjoint components with respect to the plane  $z = 0$  (the base plane). Note that for the same color, different points are obtained, corresponding to different assembly modes.

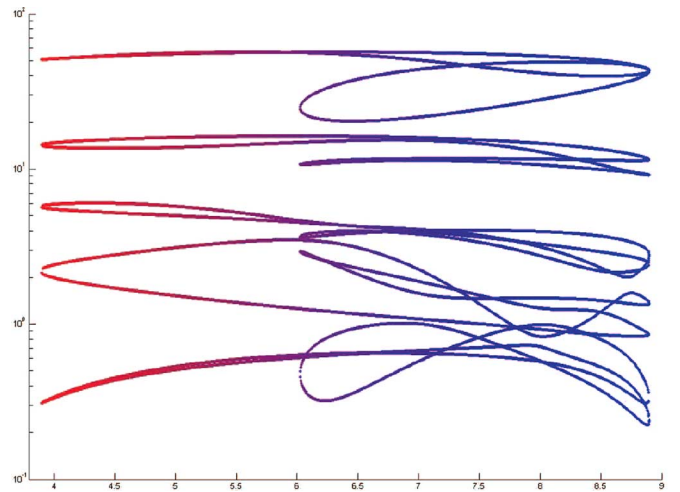


Fig. 12. All eigenvalues for all assembly modes, excluding the one that is always zero, of  $\mathbf{J}^T \mathbf{J}$ , where  $\mathbf{J}$  is the Jacobian matrix of the analyzed architecturally singular Griffis–Duffy platform, as a function of  $l_6^2$ .

In order to validate the obtained self-motions, we have compared the results, which are obtained using the proposed parameterization technique, and those obtained using the CUIK software package. CUIK uses linear relaxation techniques to discretize the space of all the configurations that a multiloop linkage can adopt [37]. The obtained results for the attachment coordinates and the leg lengths of the Griffis–Duffy manipulator in [37] (also available online in [38]) are shown in Fig. 13. For this example, details on the obtained parameterization are provided in a Maple worksheet, which is included in the attached multimedia material. The solution obtained using CUIK consists of a list of boxes approximating the self-motion with a resolution of  $10^{-3}$ . It can be checked that the sampled points obtained using the proposed technique are all included in these boxes.

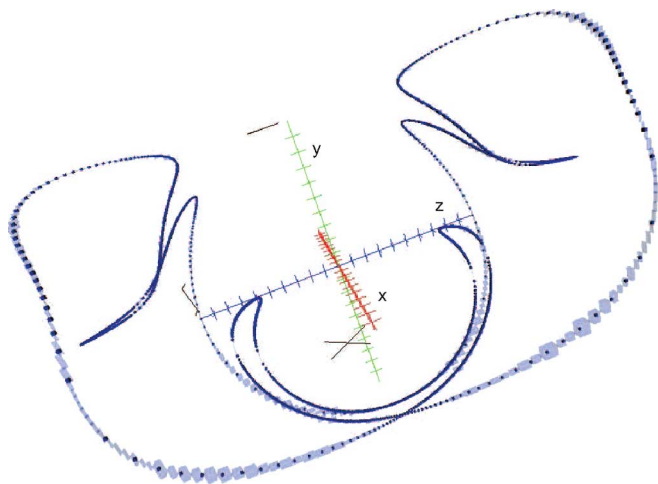


Fig. 13. Self-motion discretization of an architecturally singular Griffis–Duffy platform, which is obtained using CUIK, is plotted in light transparent blue, and the samples obtained with the presented parameterization are in dark blue.

## VI. FURTHER APPLICATION CONTEXT

The aim of this paper is to define the concept of  $\Delta$ -transform, as well as to explain the details of its usage, thus showing how sets of such transforms can be applied sequentially and/or simultaneously.

In order to illustrate the potential of the approach, two examples have been worked out in detail, both unraveling the singularity-wise equivalence of two well-known parallel platforms (flagged and Zhang–Song, on the one hand, and octahedral and Griffis–Duffy, on the other hand), thus permitting simplification of designs by removing multiple spherical joints.

Now, let us mention that the  $\Delta$ -transform has proven useful in several other contexts. Aside from the extension of the core family of flagged manipulators [11] with some new designs [30], the interesting family of partially flagged platforms has now been derived [39], which includes the celebrated 3-2-1 Hunt–Primrose manipulator as one of its members. Of practical relevance is the synthesis of a singularity-free redundant design, which combines two members of this family, and is also free of multiple spherical joints.

Another promising application is in the context of parallel manipulators, including a 5-DOF line–plane component [40], where fruitful kinematic equivalences are currently being explored.

Needless to say, the application of the  $\Delta$ -transform to 3-DOF planar parallel manipulators is straightforward.

However, the proposed methodology goes well beyond the fully parallel Gough–Stewart platforms mentioned up to now as it applies to any parallel robot having a  $\Delta$  component or *any kinematically equivalent serial chain*. For instance, several 2-DOF serial chains, which are considered in [41], are kinematically equivalent to  $\Delta$  components, and we have exploited this fact in previous works to analyze the singularity structure of, for instance, a three-legged manipulator with  $\underline{PRPS}$  chains as legs (see, [11, Fig. 12]).

## VII. CONCLUSION

The idea of using  $\Delta$ -transforms for the kinematic analysis of parallel platforms, which is introduced in this paper, was first proposed in [11] to generate the family of flagged parallel manipulators. In this paper, we have formalized and extended this idea, thus introducing the possibility of applying sets of these transformations simultaneously. This extension permits the following:

- 1) classifying platforms in families sharing the same singularity structure;
- 2) modifying platforms, without modifying the location of their singularities, to satisfy extra design criteria (this includes the possibility of eliminating multiple spherical joints, whose implementation always introduces some complications);
- 3) characterizing self-motions associated with nontrivial architectural singularities.

With regard to the last point, note that the characterization of self-motions has important practical applications in redundant parallel robots and the emerging area of reconfigurable parallel robots. For example, a redundant parallel robot, in which its base attachments can be moved along guides [42], should be controlled in such a way that it remains far from this kind of singularities. Alternatively, one might be interested in approaching them so that the robot stiffness is reduced in a given direction to ease some tasks requiring accommodation.

A  $\Delta$ -transform essentially refers to a leg rearrangement in a  $\Delta$  component, which is a rigid subassembly involving a line and a point. Then, it is reasonable to wonder if other particular leg rearrangements exist for point–plane, line–line, or line–plane components that leave singularities invariant. The point–plane case can be easily shown to reduce to the application of two  $\Delta$ -transforms [11], while the line–line one has been shown in Section IV (see Fig. 5) of this paper to also boil down to the application of four serial followed by four simultaneous  $\Delta$ -transforms. The case of the line–plane component and, possibly, that of the general plane–plane one remain as a promising avenue of future research.

## APPENDIX

Singularities of Gough–Stewart platforms correspond to zeros of  $\det(\mathbf{P})$  in (3). It is known that the rows of matrix  $\mathbf{P}$  are the Plücker coordinates of the leg lines [3], [43]. Thus, identifying singularities amounts to finding those configurations in which the leg-lines vectors become linearly dependent. This kind of linear dependency was first treated in [44] and [45].

White [46] showed that the condition  $\det(\mathbf{P}) = 0$  could be expressed as the sum of terms involving the product of three determinants, which are termed *brackets*, the four columns of which correspond to the coordinates of four leg attachments written in homogeneous coordinates. Thus, this expression becoming zero, which is known as the *pure condition*, is equivalent to the determinant of  $\mathbf{P}$  vanishing.

There exist several equivalent expressions of the pure condition associated with the general Gough–Stewart platform.

Downing *et al.* [18] used the following 16-term expression:

$$\begin{aligned}
& [b_1 a_1 b_4 b_5][b_2 a_2 a_4 b_6][b_3 a_3 a_5 a_6] \\
& - [b_4 a_4 b_1 b_2][b_5 a_5 a_1 b_3][b_6 a_6 a_2 a_3] \\
& - [b_1 a_1 b_4 b_5][b_2 a_2 a_4 a_6][b_3 a_3 a_5 b_6] \\
& + [b_4 a_4 b_1 b_2][b_5 a_5 a_1 a_3][b_6 a_6 a_2 b_3] \\
& - [b_1 a_1 b_4 a_5][b_2 a_2 a_4 b_6][b_3 a_3 b_5 a_6] \\
& + [b_4 a_4 b_1 a_2][b_5 a_5 a_1 b_3][b_6 a_6 b_2 a_3] \\
& + [b_1 a_1 b_4 a_5][b_2 a_2 a_4 a_6][b_3 a_3 b_5 b_6] \\
& - [b_4 a_4 b_1 a_2][b_5 a_5 a_1 a_3][b_6 a_6 b_2 b_3] \\
& - [b_1 a_1 a_4 b_5][b_2 a_2 b_4 b_6][b_3 a_3 a_5 a_6] \\
& + [b_4 a_4 a_1 b_2][b_5 a_5 b_1 b_3][b_6 a_6 a_2 a_3] \\
& + [b_1 a_1 a_4 b_5][b_2 a_2 b_4 a_6][b_3 a_3 a_5 b_6] \\
& - [b_4 a_4 a_1 b_2][b_5 a_5 b_1 a_3][b_6 a_6 a_2 b_3] \\
& + [b_1 a_1 a_4 a_5][b_2 a_2 b_4 b_6][b_3 a_3 b_5 a_6] \\
& - [b_4 a_4 a_1 a_2][b_5 a_5 b_1 b_3][b_6 a_6 b_2 a_3] \\
& - [b_1 a_1 a_4 a_5][b_2 a_2 b_4 a_6][b_3 a_3 b_5 b_6] \\
& + [b_4 a_4 a_1 a_2][b_5 a_5 b_1 a_3][b_6 a_6 b_2 b_3] = 0 \quad (34)
\end{aligned}$$

while Ben-Horin and Shoham [47] used the following 24-term expression instead:

$$\begin{aligned}
& [b_1 a_1 b_2 a_2][b_3 a_3 b_4 b_5][a_4 a_5 b_6 a_6] \\
& - [b_1 a_1 b_2 a_2][b_3 a_3 a_4 b_5][b_4 a_5 b_6 a_6] \\
& - [b_1 a_1 b_2 a_2][b_3 a_3 b_4 a_5][a_4 b_5 b_6 a_6] \\
& + [b_1 a_1 b_2 a_2][b_3 a_3 a_4 a_5][b_4 b_5 b_6 a_6] \\
& - [b_1 a_1 b_2 b_3][a_2 a_3 b_4 a_4][b_5 a_5 b_6 a_6] \\
& + [b_1 a_1 a_2 b_3][b_2 a_3 b_4 a_4][b_5 a_5 b_6 a_6] \\
& - [b_1 a_1 a_2 a_3][b_2 b_3 b_4 a_4][b_5 a_5 b_6 a_6] \\
& + [b_1 a_1 b_2 a_3][a_2 b_3 b_4 a_4][b_5 a_5 b_6 a_6] \\
& - [b_1 a_1 b_2 b_3][a_2 b_4 a_4 b_5][a_3 a_5 b_6 a_6] \\
& + [b_1 a_1 a_2 b_3][b_2 b_4 a_4 b_5][a_3 a_5 b_6 a_6] \\
& - [b_1 a_1 a_2 a_3][b_2 b_4 a_4 b_5][b_3 a_5 b_6 a_6] \\
& + [b_1 a_1 b_2 a_3][a_2 b_4 a_4 b_5][b_3 a_5 b_6 a_6] \\
& + [b_1 a_1 b_2 b_3][a_2 b_4 a_4 a_5][a_3 b_5 b_6 a_6] \\
& - [b_1 a_1 a_2 b_3][b_2 b_4 a_4 a_5][a_3 b_5 b_6 a_6] \\
& + [b_1 a_1 a_2 a_3][b_2 b_4 a_4 a_5][b_3 b_5 b_6 a_6] \\
& - [b_1 a_1 b_2 a_3][a_2 b_4 a_4 a_5][b_3 b_5 b_6 a_6] \\
& + [b_1 a_1 b_2 b_4][a_2 b_3 a_3 b_5][a_4 a_5 b_6 a_6] \\
& - [b_1 a_1 b_2 a_4][a_2 b_3 a_3 b_5][b_4 a_5 b_6 a_6] \\
& - [b_1 a_1 a_2 b_4][b_2 b_3 a_3 b_5][a_4 a_5 b_6 a_6]
\end{aligned}$$

$$\begin{aligned}
& + [b_1 a_1 a_2 a_4][b_2 b_3 a_3 b_5][b_4 a_5 b_6 a_6] \\
& - [b_1 a_1 b_2 b_4][a_2 b_3 a_3 a_5][a_4 b_5 b_6 a_6] \\
& + [b_1 a_1 b_2 a_4][a_2 b_3 a_3 a_5][b_4 b_5 b_6 a_6] \\
& + [b_1 a_1 a_2 b_4][b_2 b_3 a_3 a_5][a_4 b_5 b_6 a_6] \\
& - [b_1 a_1 a_2 a_4][b_2 b_3 a_3 a_5][b_4 b_5 b_6 a_6] = 0 \quad (35)
\end{aligned}$$

where  $a_i$  and  $b_i$  are the homogeneous coordinates of the attachments  $\mathbf{a}_i$  and  $\mathbf{b}_i$ , respectively, for  $i = 1, \dots, 6$ . In other words,  $a_i = (\mathbf{a}_i^T, 1)^T$ , and  $b_i = (\mathbf{b}_i^T, 1)^T$  (see Fig. 2).

The advantage of using the previous expressions to represent the dependence of leg lines is seen when investigating simplified forms of the general Stewart–Gough platform in which, for example, some legs share attachments. In general, placing constraints on the geometrical structure of the platform reduces the number of bracket terms to a manageable level, thus offering the opportunity for simple geometrical interpretations of the singularities. For example, since a bracket involving the same point at least twice is zero, the pure condition of a platform in which several attachments coincide is greatly simplified. Although using either (34) or (35) to obtain the simplified forms of the pure condition is fully equivalent, the result might be more compact in one case than in the other, thus avoiding the need of further algebraic manipulations for its simplification. For instance, for the octahedral manipulator, which is shown in the right-hand side of Fig. 3, (34) reduces directly to the pure condition in (5), and for the manipulator, which is shown in the left-hand side of Fig. 3, (35) simplifies directly to the pure condition in (4).

#### ACKNOWLEDGMENT

The authors would like to thank J. M. Porta for his help in using the CUIK software package for the validation of the proposed method to parameterize self-motions.

#### REFERENCES

- [1] P. Donelan. (2007). Singularities in robot kinematic—A publications database [Online]. Available: <http://www.mcs.vuw.ac.nz/~donelan/cgi-bin/rs/main>
- [2] K. Hunt, “Structural kinematics of in-parallel actuated robot arms,” *ASME J. Mechanisms, Transmiss., Autom. Des.*, vol. 105, pp. 705–712, 1983.
- [3] J.-P. Merlet, “Singular configurations of parallel manipulators and Grassmann geometry,” *Int. J. Robot. Res.*, vol. 8, no. 5, pp. 45–56, 1989.
- [4] C. Gosselin and J. Angeles, “Singularity analysis of closed-loop kinematic chains,” *IEEE Trans. Robot.*, vol. 6, no. 3, pp. 281–290, Jun. 1990.
- [5] V. Kumar, “Instantaneous kinematics of parallel-chain robotic mechanisms,” *J. Mech. Des.*, vol. 114, pp. 349–358, 1992.
- [6] X. Kong and C. Gosselin, “Classification of 6-SPS parallel manipulators according to their components,” presented at the Amer. Soc. Mech. Eng. Des. Eng. Tech. Conf. (DETC 2000/MECH-14105), Baltimore, MD, 2000.
- [7] J. Borràs, F. Thomas, and C. Torras, “Analysing the singularities of 6-SPS parallel robots using virtual legs,” in *Proc. 2nd Int. Workshop Fundam. Issues Future Res. Directions Parallel Mechanisms Manipulators*, 2008, pp. 145–150.
- [8] M. Husty, S. Mielczarek, and M. Hiller, “A redundant spatial Stewart–Gough platform with a maximal forward kinematics solution set,” in *Proc. Int. Symp. Adv. Robot Kinematics*, 2002, pp. 147–154.
- [9] N. Simaan and M. Shoham, “Singularity analysis of a class of composite serial in-parallel robots,” *IEEE Trans. Robot. Autom.*, vol. 17, no. 3, pp. 301–311, Jun. 2001.
- [10] H. Pottmann and J. Wallner, *Computational Line Geometry*. Berlin, Germany: Springer-Verlag, 2001.

- [11] M. Alberich-Carramiñana, F. Thomas, and C. Torras, "Flagged parallel manipulators," *IEEE Trans. Robot.*, vol. 23, no. 5, pp. 1013–1023, Oct. 2007.
- [12] O. Ma and J. Angeles, "Architecture singularities of platform manipulators," in *Proc. IEEE Int. Conf. Robot. Autom.*, 1991, vol. 2, pp. 1542–1547.
- [13] A. Karger and M. Husty, "Singularities and self-motions of Stewart-Gough platforms," in *Proc. Comput. Methods Mechanisms, NATO Adv. Study Inst.*, 1997, pp. 279–288.
- [14] A. Karger, "New self-motions of parallel manipulators," in *Proc. Int. Symp. Adv. Robot Kinematics*, 2008, pp. 275–282.
- [15] A. J. Sommese, J. Verschelde, and C. Wampler, "Advances in polynomial continuation for solving problems in kinematics," *J. Mech. Des.*, vol. 126, no. 2, pp. 262–268, 2004.
- [16] A. J. Sommese and C. Wampler, *The Numerical Solution of Systems of Polynomials Arising in Engineering and Science*. Singapore: World Scientific, 2005.
- [17] J.-P. Merlet and P. Donelan, "On the regularity of the inverse jacobian of parallel robots," in *Proc. Int. Symp. Adv. Robot Kinematics*, 2006, pp. 41–48.
- [18] D. Downing, A. Samuel, and K. Hunt, "Identification of the special configurations of the octahedral manipulator using the pure condition," *Int. J. Robot. Res.*, vol. 21, pp. 147–159, 2002.
- [19] H. Dörrie, *100 Great Problems of Elementary Mathematics. Their History and Solution*. New York: Dover, 1965.
- [20] D. Michelucci and S. Foufouy, "Using Cayley–Menger determinants for geometric constraint solving," in *Proc. ACM Symp. Solid Model. Appl.*, 2004, pp. 285–290.
- [21] G. M. Crippen and T. F. Havel, *Distance Geometry and Molecular Conformation*. Taunton, U.K.: Res. Studies, 1988.
- [22] F. Thomas and L. Ros, "Revisiting trilateration for robot localization," *IEEE Trans. Robot.*, vol. 21, no. 1, pp. 93–101, Feb. 2005.
- [23] J. M. Porta, L. Ros, F. Thomas, and C. Torras, "A branch-and-prune solver for distance constraints," *IEEE Trans. Robot.*, vol. 21, no. 2, pp. 176–187, Apr. 2005.
- [24] C. Zhang and S. Song, "Forward kinematics of a class of parallel (Stewart) platforms with closed-form solutions," in *Proc. IEEE Int. Conf. Robot. Autom.*, 1991, pp. 2676–2681.
- [25] J. Milne, *An Elementary Treatise on Cross-Ratio Geometry with Historical Notes*. Cambridge, U.K.: Cambridge Univ. Press, 1911.
- [26] X. Kong, "Generation of singular 6-SPS parallel manipulators," presented at the Amer. Soc. Mech. Eng. Des. Eng. Tech. Conf. (DETC 1998/MECH-5952), Atlanta, GA, 1998.
- [27] M. Husty and A. Karger, "Architecture singular parallel manipulators and their self-motions," in *Proc. Int. Symp. Adv. Robot Kinematics*, 2000, pp. 355–364.
- [28] A. Karger, "Architecturally singular non-planar parallel manipulators," *Mechanism Mach. Theory*, vol. 43, pp. 335–346, 2008.
- [29] P. Ben-Horin and M. Shoham, "Singularity of Gough–Stewart platforms with collinear joints," in *Proc. 12th IFToMM World Congr.*, 2007, pp. 18–21.
- [30] J. Borràs, F. Thomas, and C. Torras, "Architecture singularities in flagged parallel manipulators," in *Proc. IEEE Int. Conf. Robot. Autom.*, 2008, pp. 3844–3850.
- [31] M. Griffis and J. Duffy, "Method and apparatus for controlling geometrically simple parallel mechanisms with distinctive connections," U.S. Patent 5 179 525, Jan. 12, 1993.
- [32] M. Husty and A. Karger, "Self-motions of Griffis–Duffy type parallel manipulators," in *Proc. IEEE Int. Conf. Robot. Autom.*, 2000, pp. 7–12.
- [33] Y. Zhu, L. Senevirante, and S. Earles, "A new structure of invariant for 3d point sets from a single view," in *Proc. IEEE Int. Conf. Robot. Autom.*, 1995, pp. 1726–1731.
- [34] K. Wohlhart, "Mobile 6-SPS parallel mainpulators," *J. Robot. Syst.*, vol. 20, no. 8, pp. 509–516, 2003.
- [35] A. Karger, "Architecture singular planar parallel manipulators," *Mechanism Mach. Theory*, vol. 38, pp. 1149–1164, 2003.
- [36] L.-W. Tsai, *Robot Analysis. The Mechanics of Serial and Parallel Manipulators*. New York: Wiley, 1999.
- [37] J. Porta, L. Ros, and F. Thomas, "A linear relaxation technique for the position analysis of multiloop linkages," *IEEE Trans. Robot.*, vol. 25, no. 2, pp. 225–239, Apr. 2009.
- [38] The CUIK project. (2009). [Online]. Available: <http://www-iri.upc.es/groups/gmr/cuikweb>
- [39] M. Alberich-Carramiñana, M. Garolera, F. Thomas, and C. Torras, "Partially-flagged parallel manipulators: Singularity charting and avoidance," *IEEE Trans. Robot.*, vol. 25, no. 4, pp. 771–784, Aug. 2009.
- [40] J. Borràs and F. Thomas, "Kinematics of line–plane subassemblies in Stewart platforms," in *Proc. IEEE Int. Conf. Robot. Autom.*, 2009, pp. 4094–4099.
- [41] P. Ben-Horin and M. Shoham, "Singularity condition of six degree-of-freedom three-legged parallel robots based on Grassmann–Cayley algebra," *IEEE Trans. Robot.*, vol. 22, no. 4, pp. 577–590, Aug. 2006.
- [42] J. Borràs, F. Thomas, E. Ottaviano, and M. Ceccarelli, "Reconfigurable 5-DOF 5-SPU parallel platform," *ASME/IFToMM Int. Conf. Reconfigurable Mechanisms Robots*, London: King's College, London, U.K., 2009.
- [43] B. M. St-Onge and C. Gosselin, "Singularity analysis and representation of the general Gough–Stewart platform," *Int. J. Robot. Res.*, vol. 19, no. 3, pp. 271–288, 2000.
- [44] A. Dandurand, "The rigidity of compound spatial grids," *Struct. Topol.*, vol. 10, pp. 41–56, 1984.
- [45] C. Gibson and K. Hunt, "Geometry of screw systems II, screws: Classification of screw systems," *Mechanism Mach. Theory*, vol. 25, no. 1, pp. 11–27, 1990.
- [46] N. White, "The bracket of 2-extensors," *Congressus Numerantium*, vol. 40, pp. 419–428, 1983.
- [47] P. Ben-Horin and M. Shoham, "Application of Grassmann–Cayley algebra to geometrical interpretation of parallel robot singularities," *Int. J. Robot. Res.*, vol. 28, no. 1, pp. 127–141, 2009.



**Júlia Borràs** received the M.Sc. degree in mathematics from the Universitat Politècnica de Catalunya, Barcelona, Spain, in 2004 and the B.Sc. degree in computer science from the Open University of Catalonia, Barcelona, in 2006. She is currently working toward the Ph.D. degree with the Institut de Robòtica i Informàtica Industrial, Barcelona.

From 2004 to 2007, she was a Programmer with several companies.



**Federico Thomas** (M'06) received the Telecommunications Engineering degree and the Ph.D. degree in computer science, both from the Universitat Politècnica de Catalunya, Barcelona, Spain, in 1984 and 1988, respectively.

He is currently a Research Professor with the Institut de Robòtica i Informàtica Industrial, Consejo Superior de Investigaciones Científicas, Barcelona. His current research interests include geometry and kinematics with applications to robotics, computer graphics, and computer vision.

Prof. Thomas is an Associate Editor of the IEEE TRANSACTIONS ON ROBOTICS.



**Carme Torras** (M'07) received the M.Sc. degrees in mathematics and computer science from the Universitat de Barcelona, Barcelona, Spain, and the University of Massachusetts, Amherst, respectively, and the Ph.D. degree in computer science from the Universitat Politècnica de Catalunya, Barcelona.

She is currently a Research Professor with the Consejo Superior de Investigaciones Científicas, Barcelona. She has authored or coauthored five books and about 200 papers in the areas of robot kinematics, geometric reasoning, computer vision, and neurocomputing. She has been a local Project Leader of several European projects, such as "Planning Robot Motion," "Robot Control Based on Neural Network Systems," "Self-organization and Analogical Modelling Using Subsymbolic Computing," "Behavioural Learning: Sensing and Acting," and the ongoing sixth framework IP project "Perception, Action, and Cognition Through Learning of Object–Action Complexes."